ingegneria sismica
International Journal of Earthquake Engineering
Anno XLIII - Num. 1 - 2026

Sensitivity analysis and optimal design of tensioned monolithic structure stiffness matrix under different loads

Yingyu Zhao[1,*], *Ani Luo*[1] *and Heping Liu*[1]

[1] College of Mechanical and Electrical Engineering, Harbin Engineering University, Harbin, Heilongjiang, 150001, China

SUMMARY: *In this study, through a scheme combining theoretical analysis, numerical simulation and optimization algorithm, the influence law of different load acting positions on the structural stiffness matrix is investigated, and a multi-objective topology optimization design framework based on the genetic algorithm of small habitats is proposed. Firstly, the tensioned overall structural stiffness matrix is derived, which leads to the judgment conditions of the tensioned overall structural stability and zero-stiffness displacement mode. The optimization objective is set to minimize the total mass of the structure, and the topology optimization of the tensioned overall structure is carried out. The shared function small habitat technique and pre-selection mechanism are adopted to solve the stable modes of the tensioned monolithic structure under different conditions. Then the nonlinear evolution characteristics of nodal displacement and stiffness under various typical loads are analyzed using a quadrangular tensile monolithic structure as the research object. The evaluation results revealed that the structure with a grouping number of 12 has an optimal overall performance with a percentage area of 59.25%. At the same time, the structure with this grouping is also the structure with the lowest sensitivity and the strongest robustness, which indicates that the optimization strategy in this paper effectively designs the tensioned monolithic structure with high structural adaptability. This study provides theoretical basis and methodological support for the design and optimization of the performance of tensioned monolithic structures under different loading environments.*

KEYWORDS: *Tensioned monolithic structure; topology optimization; small habitat genetic algorithm; stiffness matrix; sensitivity analysis*

1 Introduction

Tensioned monolithic structure, as a new type of prestressed large-span structure, has developed rapidly in the field of space structure in recent years [1]. Tensioned monolithic structure, a unique self-equilibrium structural system composed of a set of continuous tension members and a set of discontinuous compression members, is a kind of flexible and large deformation space structure with special force, whose stiffness is provided by the flexible cable elements in tension and the rigid rod elements in compression [2, 3]. The advantages of tensile monolithic structure are mainly variable stiffness, reasonable force, controllable morphology, light weight, and folding and spreading, etc. Its different characteristics from traditional structures have received extensive attention in the fields of architectural space structure, aerospace folding and spreading structure, intelligent robotics, and biomedicine, etc. [4, 5]. Tension integration perfectly shows

*zhaoyingyu2025@163.com
https://doi.org/10.65102/is2026017
Published: 30 April, 2026

the objective law of “continuous tension and intermittent compression” of the nature of the tensile integral structure, and because the force mode of the tensile integral structure is very reasonable, it can make up for the deficiencies of the traditional space structure such as mesh shell structure and mesh frame structure in the design of the large-span space structure [6-8]. However, due to the fact that the tensile integral structure belongs to the flexible large deformation structure, its stiffness is very easy to be affected by the intrinsic factors or extrinsic conditions, and the actual building structure has not been widely used in the real sense of the tensile integral system [9, 10]. It is of great significance to study the influence of different loads on the stiffness of the tensile integral structure, and to analyze and optimize the design of its stiffness for the application of the tensile integral structure in actual construction projects.

At present, scholars in various fields of academia conduct major studies on mechanical analysis, shape finding analysis, structural topology analysis and stiffness analysis of tensile monolithic structures. In terms of mechanical properties analysis, Gilewski et al [11] investigated the equivalent mechanical properties of tensioned monolithic structures, used the continuum model to comprehensively analyze five typical tensioned monolithic structures with different properties, determined their Young's modulus, shear modulus, Poisson's ratio and other effectiveness properties, and visually presented the relationship between their mechanical coefficients and self-stress multiplicity and the performance ratio of the cords and rods. Ali et al [12] systematically analyzed the dynamic characteristics and vibration control strategy of the tensioned monolithic on the vibration control can change the self-stress level of the tensioned monolithic structure, it was found that the control of the self-stress can affect the dynamic performance of the tensioned monolithic structure, and then the vibration control strategy with the minimum control cost was obtained by using the PGSL stochastic search algorithm.

In terms of structural shape finding analysis, Tran et al [13] proposed a numerical method for a new self-equilibrium configuration of tensile monolithic structures by eigenvalue decomposition of force density matrix and singular value decomposition of equilibrium matrix in order to obtain feasible sets of node coordinates and force densities that satisfy the minimum requirement of rank defects, which is a method that has a better robustness in the arithmetic test. Lee, S et al [14] proposed a generalized shape finding procedure for truncated polyhedral tensile monolithic structures using the force density method combined with genetic algorithms, where multiple force density curves are obtained by exploring the constraint minimization problem and compared with truncated tetrahedra, dodecahedra and icosahedra in order to find feasible self-equilibrating stable configurations. Zhang, P et al [15] established an optimization model for the forming of tensioned monolithic structures by taking the self-equilibrium equations of tensioned monolithic structures as the optimal performance condition, and used dynamic relaxation technique based on kinetic damping to find the optimal solution set, and the numerical simulation results proved that the method has a powerful searching ability for finding the shape of tensioned monolithic structures. Cai et al [16] pointed out that finding parallel configurations is of great significance in the design of tensioned monolithic structures, and this process is known as structural shape finding, for this reason, an efficient shape finding method is proposed, and in the design of planar and spatial tensioned monolithic structures the results obtained by this method are in agreement with those obtained by the previous studies. Gasparini et al [17] investigated a mathematical model for shape finding and static analysis of tensile monolithic structures, they considered shape finding and static analysis an unconstrained nonlinear programming problem with the total potential energy as the objective function, and the validity of the proposed method for shape finding and static analysis was verified by numerical comparative experiments. Yuan et al [18] used the topology, initial configuration, rest length and axial stiffness of the units of the tensioned monolithic structure as the input parameters of the method for solving the nonlinear equilibrium equations to find the shape, and

realized the shape finding of the tensioned monolithic structure by solving a nonlinear least squares problem, which showed excellent accuracy and effectiveness.

In terms of structural topology analysis, Wang et al [19] used a linear optimization algorithm to optimize the topology of the tensioned monolithic structure under the constraints of equilibrium conditions, member yielding, cable relaxation, support buckling, and node displacement, and the method reduces the material consumption of the optimized design of the topology, and obtains a lighter weight tensioned monolithic structure. Xu et al [20] constructed an optimization model with member connections and member internal forces as variable phases, and used the ground structure method to find a self-stressing tensioned monolithic structure under multiple constraints, and the method used to find a wider range of tensioned monolithic structures after solving the topological optimization problem by a mixed integer linear algorithm. Liu et al [21] proposed a method for the optimal design of the topology of a tensioned monolithic structure based on graph theory, which geometrically provides the topology of the tension of each bar within the shape of the structure, and the resulting structural tensions tend to be both stable and symmetric. Ehara et al [22] implemented the topological design of the tensioned monolithic structure based on a mixed integer programming algorithm, and the study identified the maximization of the number of rods and the minimization of the number of cables as the optimization solution problem, based on which the obtained tensioned monolithic structure strictly meets the discontinuity requirements of the rods. Feng et al [23] designed a format matrix algorithm for 0 and -1 topological codes in order to obtain topological forms of tensile monolithic structures with a variety of self-stressing modes. The algorithm encodes the structural components and then generates the scheme matrix under geometric constraints, and the resulting structure performs well in terms of stiffness, elastic strain, and so on. Lee, S et al [24] proposed a topology design scheme for tensioned monolithic structures by combining the force density method with a genetic algorithm, using discontinuity conditions and minimum tensioned monolithic structures respectively in order to select the support candidate groups, and the arithmetic example proved that the proposed method has a good performance of the topology design of tensioned monolithic structures.

In terms of structural stiffness analysis, Zhang, L et al [25] proposed an efficient shape finding method based on the structural stiffness matrix of the tensioned monolithic structure, which induces the shape of the tensioned monolithic structure to converge to a stable state by the structural stiffness matrix and the total potential energy, which is also effective in coping with the large-scale regular or irregular tensioned monolithic structures. Boehler et al [26] proposed two control methods for the cable-driven tensioned monolithic structure by adjusting the prestress level of the cable rod units in the tensioned monolithic structure, thus converting the tensioned monolithic structure into a structural device with variable stiffness, and verified their control efficiency by experiments respectively. Ashwear et al [27] studied the stiffness optimization problem of tensile monolithic structures, under the comprehensive consideration of axial and transverse vibration of members, the stiffness measurement simulation was carried out by using nonlinear Euler-Bernoulli beam units, and then the multi-objective function for the optimization of the stiffness indexes was designed and solved by using genetic algorithms with a combination of multi-objective criterion, and the optimal solution with high stiffness was obtained in the end. Luo et al [28] established a data model of the tensioned monolithic structure based on the generalized node coordinates and connection matrix, and analyzed its stiffness matrix to obtain that the preload force, Young's modulus and cross-sectional area are the key elements leading to the deformation of the tensioned monolithic structure, which provides a reference to the design of the tensioned monolithic structure in the related projects. Yildiz et al [29] designed a special measurement method for the stiffness characteristics of tensioned monolithic structures, and verified the validity of the stiffness characteristics obtained by the

method in nonlinear finite element analysis, which greatly reduced the cost of calculating the tensioned monolithic structures by the obtained characteristics, and could assess the stiffness of the structures in a simpler and scientific way. Zappetti et al [30] proposed a novel design method for variable stiffness tensioned monolithic structures by utilizing the property of variable stiffness of tensioned monolithic structures as a design principle for soft robots, and proved that the proposed method has the function of dynamically adjusting the load carrying capacity and can self-drive unfolding and locking of the structure shape through different tensioned structure verification tests.

In this paper, the judgment basis of structural stiffness matrix and stability is established, which lays the foundation for investigating the node displacement and stiffness evolution law under different loading positions. Habitat genetic algorithm is introduced to construct a topology optimization model with the minimum total mass of the structure as the objective function to realize the solution of different structural equilibrium states. At the same time, this paper also adopts different groupings to calculate the initial state of the new tensioned monolithic structure, and applies examples to verify the rationality of the structure, which enriches the analysis theory and application practice of the existing tensioned monolithic structure form. Finally, through the parameter sensitivity analysis method, it reveals the sensitivity degree and robustness difference of different grouped structures to the weight coefficients.

2 Tensioned monolithic structural elements and their characteristics

2.1 Tensioned monolithic structural units and polyhedral geometry

2.1.1 Polyhedral geometry

A polyhedron is a geometric body enclosed by several polygons according to certain rules. The faces of a polyhedron are the polygons enclosing the polyhedron, the prongs of a polyhedron are the edges common to both faces, and the vertices of a polyhedron are the vertices common to a number of faces. If we denote the number of faces, the number of edges of the prisms, and the number of vertices of a polyhedron by f, m, and n, respectively, we have, according to Euler's formula:

$$f - m + n = 2 \tag{1}$$

A polyhedron is called a positive polyhedron if it consists of congruent positive polygons and each corner is a congruent polyhedral angle. There are very few species of positive polyhedra, only five, namely, positive tetrahedron, positive hexahedron, positive octahedron, positive dodecahedron, and positive icosahedron, which have been exhaustively studied in topology. In the existing structural systems, most of the structural units are several basic polyhedra and their combinations. Among these basic polyhedra and their combinations, triangular cones in tetrahedra, tetragonal cones and trigonal prisms in pentahedra, and tetragonal prisms in hexahedra are the main forms of structural units.

2.1.2 Basic polyhedral tensioned monolithic structural units

The second column of basic tensile monolithic structural units can be obtained by rotating the upper planes of the first column of prismatic prisms of prismatic tensile monolithic structural units by an α angle, and each basic tensile monolithic structural unit corresponds to a unique

α angle, which can be expressed by Eq:

$$\alpha = \frac{\pi}{2} - \frac{\pi}{n} \tag{2}$$

n is the number of sides of the upper and lower polygons, and knowing the α angles uniquely determines the basic shape of the tensile monolithic structural unit.

2.1.3 Example analysis

Figure 1 shows a quadrangular unit, the coordinate origin is located at the center of the bottom quadrilateral, the counterclockwise rotation is positive, the top and bottom planes are rotated by an angle of α with respect to the original position, and the top plane is free to rotate in the positive direction of the Z-axis. Let the angle be 0 degrees in the positive direction of X, the quadrilateral has a bottom side length of a, a top side length of b, a height of h, a diagonal cable length of L_t, and a rod length of L_s, then:

$$\alpha = \frac{\pi}{2} - \frac{\pi}{n} = \frac{\pi}{2} - \frac{\pi}{4} = \frac{\pi}{4} \tag{3}$$

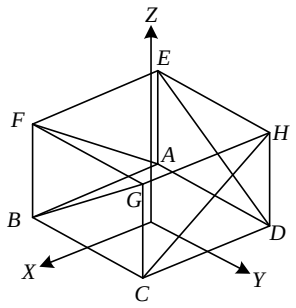

Figure 1: Four prism unit

From this, the coordinates of each node can be obtained:

$$\begin{aligned}
&A\left[-\frac{1}{2}a,-\frac{1}{2}a,0\right] \quad B\left[\frac{1}{2}a,-\frac{1}{2}a,0\right] \\
&C\left[\frac{1}{2}a,\frac{1}{2}a,0\right] \qquad D\left[-\frac{1}{2}a,\frac{1}{2}a,0\right] \\
&E\left[-\frac{\sqrt{2}}{2}b\cos\left(\frac{\pi}{4}+\alpha\right),-\frac{\sqrt{2}}{2}b\sin\left(\frac{\pi}{4}+\alpha\right),h\right] \\
&F\left[\frac{\sqrt{2}}{2}b\sin\left(\frac{\pi}{4}+\alpha\right),-\frac{\sqrt{2}}{2}b\cos\left(\frac{\pi}{4}+\alpha\right),h\right] \\
&G\left[\frac{\sqrt{2}}{2}b\cos\left(\frac{\pi}{4}+\alpha\right),\frac{\sqrt{2}}{2}b\sin\left(\frac{\pi}{4}+\alpha\right),h\right] \\
&H\left[-\frac{\sqrt{2}}{2}b\sin\left(\frac{\pi}{4}+\alpha\right),\frac{\sqrt{2}}{2}b\cos\left(\frac{\pi}{4}+\alpha\right),h\right]
\end{aligned} \tag{4}$$

Bringing in $\alpha = \frac{\pi}{4}$ gives the coordinates of the nodes as:

$$\begin{aligned} &A\left[-\frac{1}{2}a,-\frac{1}{2}a,0\right]\ B\left[\frac{1}{2}a,-\frac{1}{2}a,0\right]\ C\left[\frac{1}{2}a,\frac{1}{2}a,0\right] \\ &D\left[-\frac{1}{2}a,\frac{1}{2}a,0\right]\ E\left[0,-\frac{\sqrt{2}}{2}b,h\right]\ F\left[\frac{\sqrt{2}}{2}b,0,h\right] \\ &G\left[0,\frac{\sqrt{2}}{2}b,h\right]\ H\left[-\frac{\sqrt{2}}{2}b,0,h\right] \end{aligned} \tag{5}$$

Then the lengths of the compression bar and the diagonal cable are:

$$\begin{aligned} L_s &= \frac{\sqrt{2}}{2}\sqrt{b^2+\sqrt{2}ab+a^2+2h^2} \\ L_t &= \frac{\sqrt{2}}{2}\sqrt{b^2-\sqrt{2}ab+a^2+2h^2} \end{aligned} \tag{6}$$

2.2 Stiffness matrix and stability conditions for tensioned monolithic structures

2.2.1 Establishment of the stiffness matrix

Suppose that a small perturbation $\delta f = [\delta f_1\ \delta f_2\ \ldots\ \delta f_n]$ acting on a node of a tensile monolithic structure corresponds to a small displacement of the node $\delta d = [\delta d_1\ \delta d_2\ \ldots\ \delta d_n]$. Then:

$$\delta f = K\delta d \tag{7}$$

K is the stiffness matrix of the tensioned monolithic structure. The so-called stiffness refers to the individual external forces required to produce a unit displacement, specifically, so that the system produces a unit displacement only in the j th coordinate, it is necessary to add the appropriate force in each coordinate direction, and the external force required to be added in the i th coordinate is defined as the stiffness coefficient K_{ij}. The stiffness matrix K is decomposed into two parts according to the characteristics of the tensioned monolithic structure:

$$K = K_c + K_p \tag{8}$$

where K_c is the regular component determined by the shape of the structure before the structure is prestressed and K_p is the stress component due to prestressing.

Equilibrium equations are established at points 1 and 2:

$$\begin{cases} f_1 = nt \\ f_2 = -nt \end{cases} \tag{9}$$

where n is the directional cosine. Let the internal force coefficient $\hat{t} = t / l$; then equation (9) can be written as:

$$\begin{aligned} f_1 &= (X_1 - X_2) \times \hat{t} \\ f_2 &= (-X_1 + X_2) \times \hat{t} \end{aligned} \tag{10}$$

The K_{ij} is the external force that needs to be applied at the i th coordinate to make the system produce a unit displacement at the j th coordinate only. This is obtained from the definition of the stiffness matrix:

$$K_{11} = \frac{\partial f_1}{\partial x_1} \quad K_{12} = \frac{\partial f_1}{\partial x_2} \quad K_{21} = \frac{\partial f_2}{\partial x_1} \quad K_{22} = \frac{\partial f_2}{\partial x_2} \tag{11}$$

$$\begin{aligned} \frac{\partial f_1}{\partial x_1} &= (x_1 - x_2)\frac{\partial \hat{t}}{\partial x_1} + \hat{t} \quad \frac{\partial f_1}{\partial x_2} = (x_1 - x_2)\frac{\partial \hat{t}}{\partial x_2} - \hat{t} \\ \frac{\partial f_2}{\partial x_1} &= (-x_1 + x_2)\frac{\partial \hat{t}}{\partial x_1} - \hat{t} \quad \frac{\partial f_2}{\partial x_2} = (-x_1 + x_2)\frac{\partial \hat{t}}{\partial x_2} + \hat{t} \end{aligned} \tag{12}$$

Among them:

$$\frac{\partial \hat{t}}{\partial x_1} = \frac{\partial \hat{t}}{\partial l}\frac{\partial l}{\partial x_1} \quad \frac{\partial \hat{t}}{\partial x_2} = \frac{\partial \hat{t}}{\partial l}\frac{\partial l}{\partial x_2} \tag{13}$$

The $\frac{\partial l}{\partial x_1}$ is the component in the rod direction of the displacement generated in the x_1 coordinates. Thus it is obtained:

$$\frac{\partial l}{\partial x_1} = n \quad \frac{\partial l}{\partial x_2} = -n \tag{14}$$

Because:

$$\frac{\partial \hat{t}}{\partial l} = \frac{d\hat{t}}{dl} = \frac{d\left(\frac{t}{l}\right)}{dl} = \frac{1}{l}\frac{dt}{dl} - \frac{t}{l^2} = \frac{1}{l}\left(\frac{dt}{dl} - \hat{t}\right) \tag{15}$$

Let $g = \frac{dt}{dl}$ and bring it into the above equation to obtain:

$$\frac{\partial \hat{t}}{\partial l} = \frac{1}{l}\left(\frac{dt}{dl} - \hat{t}\right) = \frac{g - \hat{t}}{l} \tag{16}$$

Let $\hat{g} = g - \hat{t}$, and combine Eqs. (12), (13), (14), and (16) to obtain:

$$\begin{aligned} \frac{\partial f_1}{\partial x_1} &= n\hat{g}n + \hat{t} \quad \frac{\partial f_1}{\partial x_2} = -n\hat{g}n - \hat{t} \\ \frac{\partial f_2}{\partial x_1} &= -n\hat{g}n - \hat{t} \quad \frac{\partial f_2}{\partial x_2} = n\hat{g}n + \hat{t} \end{aligned} \tag{17}$$

Write it in matrix form to get:

$$K = \begin{bmatrix} n \\ -n \end{bmatrix} [\hat{g}] \begin{bmatrix} n^T & -n^T \end{bmatrix} + \begin{bmatrix} \hat{t} \times I & -\hat{t} \times I \\ -\hat{t} \times I & \hat{t} \times I \end{bmatrix} \tag{18}$$

where I is a 1st order unit array.

If n in is replaced by the cosine vector $N(n_X, n_Y, n_Z)$ of the rod with respect to the three axes of X, Y, Z, and I is replaced by the 3rd-order unitary array, the stiffness matrix of a single rod with 3 degrees of freedom is obtained K_s:

$$K_s = \begin{bmatrix} N \\ -N \end{bmatrix} [\hat{g}] \begin{bmatrix} N^T & -N^T \end{bmatrix} + \begin{bmatrix} \hat{t} \times I & -\hat{t} \times I \\ -\hat{t} \times I & \hat{t} \times I \end{bmatrix} \tag{19}$$

For the above equation, it can be expressed in matrix form by the equilibrium matrix A. For a single rod, N is the column vector of the equilibrium matrix A, i.e., $A_s = \begin{bmatrix} N^T & -N^T \end{bmatrix}^T$, such that $S_s = \begin{bmatrix} \hat{t} & -\hat{t} \\ -\hat{t} & \hat{t} \end{bmatrix}$ substituting into Eq. Then Eq. (19) can be expressed in the form of a matrix tensor product:

$$K_s = A_s [\hat{g}] A_s^T + S_s \otimes I \tag{20}$$

Since $\hat{g} = g - \hat{t}$, bringing Eq:

$$K_s = A_s [g] A_s^T - A_s \left[\hat{t}\right] A_s^T + S_s \otimes I \tag{21}$$

For a space structure consisting of multiple members, the stiffness of each member is integrated and expressed in matrix form to obtain:

$$K = A[G]A^T - A\left[\hat{T}\right]A^T + S \otimes I \tag{22}$$

where G is the diagonal array consisting of member stiffnesses (rigid rod $g = AE/l$, A, l are the cross-sectional area and length of the rod, and E is the modulus of elasticity). $\hat{T}$ is the diagonal array composed of internal force coefficients. Analysis of this equation shows that $A[G]A^T$ is the expression for the conventional stiffness matrix determined by geometry; $-A\left[\hat{T}\right]A^T + S \otimes I$ is the derived stiffness produced by the preloaded internal forces.

If we make $\hat{G} = G - \hat{T}$, the merger yields:

$$K = A\left[\hat{G}\right]A^T + S \otimes I \tag{23}$$

where S is the stress matrix resulting from prestressing, which has the same structure as the expression for the conventional stiffness matrix. Assuming that the two nodes of a member are i, j, then the stress matrix elements S_{ij} have the following relationship:

If $i \neq j$, then $S_{ij} = -\hat{t}_{ij}$.

If $i = j$, then $S_{ij} = \sum_k \hat{t}_{ij}$ (k is all the building blocks connected to point i).

If i is connected to j, then $S_{ij} = 0$.

2.2.2 Stability conditions

If the structure is in the position of minimum potential energy, then the structure will be in a stable state; at this time the shape of the structure corresponds to the minimum potential energy. Assuming that the structure has a deformation arbitrarily small deformation d, the work done by the internal forces of the structure is:

$$W = -f^T d = -d^T K^T d = -d^T K d \tag{24}$$

If the work done by the structural internal force is positive, the potential energy of the structure corresponding to the deformed structure shape decreases; on the contrary, if the work done by the structural internal force is negative, the potential energy of the structure corresponding to the deformed structure shape increases. Therefore, the condition that the potential energy corresponding to the shape of the structure is minimized is: $-d^T K d < 0$, i.e., the stiffness matrix K is positive definite.

When rigid body displacement occurs, the external force is zero, and for the rigid body displacement of the structure as a whole to produce the nodal displacement vector d, then $Kd = 0$; at this time, the displacement vector d corresponds to the eigenvector with zero eigenvalue of the stiffness matrix. The rigid body has 6 degrees of freedom in space, there are 6 linearly independent eigenvectors; therefore, they correspond to the 6 zero eigenvalues of the stiffness matrix. Therefore, when using the eigenvalues to determine the positivity of K, the eigenvalues corresponding to the displacement vectors of the nodes when the rigid body of the tensioned monolithic structure moves should be excluded.

Two mass blocks are fixed at each end of the rod, and the center is hinged to the base. If the masses of the two mass blocks are properly configured, the rod can hover in any position. The potential energy of the structure remains unchanged after the position of the rod is changed. Then the structure is in a state of random equilibrium; analyzed from the perspective of stiffness, the structure externally embodied stiffness is zero (except along the direction of the rod); both $Kd = 0$.

In a tensioned monolithic structure, the axial stiffness of the member $\hat{g} \gg \hat{t}$, $\hat{g} = g - \hat{t}$, $\hat{g} \approx g$, and in general $\hat{g} > 0$, the matrix $\hat{G}$ is positive definite. If there is a small deformation d_z such that $Kd_z = 0$, the stiffness of the mechanism corresponding to the d_z displacement mode is zero; the vector d_z belongs to the zero space of the stiffness matrix K. If the cable-rod tension structure is stable, the stiffness matrix K is positive definite, and the vector d_z is the eigenvector corresponding to the zero eigenvalue of the stiffness matrix K, i.e., the rigid body of the cable-rod tension structure moves.

If the cords in the structure are replaced by springs (with zero original length), then:

$$\hat{g} = t / l / l \quad \hat{t} = t / l / l \tag{25}$$

Then available:

$$\hat{g} = g - \hat{t} = 0 \tag{26}$$

At this point the matrix $\hat{G}$ is semi-positive definite. Suppose there exists a small deformation d_z such that:

$$Sd_z = 0 \tag{27}$$

The vector d_z can be a linear combination of the zero-space vectors of the stress matrix S;

$$A^T d_z = e \tag{28}$$

Bringing the vector d_z in, if there exists a nonzero solution for e, then the elements of the vector e corresponding to the deformed portion of the rigid members of the structure are zero, and the elements corresponding to the deformed portion of the spring members are nonzero.

Right-multiplication of the vector e by $\hat{G}$ yields:

$$\hat{G}e = \hat{G}A^T d_z \tag{29}$$

The nonzero elements in the vector e correspond to the zero elements in the matrix $\hat{G}$, and the zero elements in the vector e correspond to the nonzero elements in the matrix $\hat{G}$, thus:

$$\hat{G}e = 0 \tag{30}$$

Eq. (29) left-multiplied by the equilibrium matrix A is obtained by combining Eq. (30):

$$A\hat{G}A^T d_z = 0 \tag{31}$$

Then:

$$Kd_z = A\hat{G}A^T d_z + Sd_z = 0 \tag{32}$$

The zero stiffness mode condition of the structure is satisfied, i.e., $Kd_z = 0$.

If Eq. (32) holds, then d_z belongs to both the zero space of matrix $A\hat{G}A^T$ and matrix S, and it can be judged that the zero space vector of matrix $A\hat{G}A^T$ and the zero space vector of matrix S are linearly related. Suppose $W = [M \quad N]$, where M is the zero space of matrix $A\hat{G}A^T$ with rank r_M and N is the zero space of matrix S with rank r_N. Then:

$$r_W < r_M + r_N - 6 \tag{33}$$

Eq. (33) can be used to determine if there is a zero-stiffness displacement mode in the tensioned monolithic structure.

3 Topology optimization of tensioned monolithic structures based on small habitat genetic algorithms

3.1 Microhabitat genetic algorithms and structural self-equilibrium state solving

3.1.1 Shared function microhabitat techniques and pre-selection mechanisms

In this paper, the traditional genetic algorithm is improved by combining the sharing function small habitat technology and pre-selection mechanism to maintain the diversity of the population, in order to improve the stability and reliability of the algorithm.

The sharing function is used to measure the neighboring relationship and degree of two individuals, let $d_1(i, j)$ be the Heming distance of any two individuals i, j, and $d_2(i, j)$ is the fitness distance, then the sharing function $S_{i,j}$ can be defined as:

$$S_{i,j} = \begin{cases} 1 - \dfrac{d_1(i, j)}{a_1} & (d_1 < a_1, d_2 \geq a_2) \\ 1 - \dfrac{d_2(i, j)}{a_2} & (d_1 \geq a_1, d_2 < a_2) \\ 1 - \dfrac{d_1(i, j) d_2(i, j)}{a_1 a_2} & (d_1 \geq a_1, d_2 \geq a_2) \\ 0 & (Otherf) \end{cases} \tag{34}$$

where: a_1 is the maximum distance of the genotype's as an individual within a small habitat radius, and a_2 is the maximum distance of the expression's as an individual within a small habitat radius.

After sharing, the fitness function of an individual becomes the following form:

$$f_s(i) = \frac{f_i}{\sum_{j=1}^{M} S(i, j)} \tag{35}$$

where: $f_s(i)$ is the individual fitness function adjusted by the sharing function, f_i is the original individual fitness function, and M is the number of individuals in the population.

3.1.2 Solving for the self-equilibrium state of a structure

For a tensile monolithic structure under arbitrary topological conditions, this paper adopts a self-compiled stiffness matrix-based method for finding the shape of tensile monolithic structure (SMFF method) to determine its self-equilibrium state.

The SMFF method mainly contains the following steps:

1) Determine the basic data of the tensioned monolithic structure, including the number of nodes and cells, the structural topology, the initial lengths of all cells, and the axial stiffness. Using any configuration as its initial state, calculate the initial potential energy of the structure, the structural stiffness matrix, and the nodal unbalance forces. Memorize the iteration step number $N = N + 1$;

2) Select appropriate constraints to exclude the structural rigid body motion according to the random selection algorithm, determine whether the corresponding stiffness matrix is positive definite, and if it is not satisfied, use the limit step algorithm to modify the stiffness matrix so that it is positive definite;

3) Solve for the node displacements by using the stiffness matrix from step 2), and then update the node coordinates using the linear search algorithm;

4) Calculate the nodal unbalanced forces and determine whether the current state is self-equilibrium according to the convergence condition. If it is not satisfied, recalculate the structural stiffness matrix and go to step 2), otherwise, go to step 5);

5) Terminate the iteration to obtain the self-equilibrium state of the tensioned overall structure.

3.2 Topology optimization objective function and constraints

3.2.1 Establishment of the objective function

The objective function refers to the functional relationship between the objective of interest (a certain variable) and the relevant factors (some variables). According to the mechanical characteristics of the tensile monolithic structure, this paper adopts the minimum total mass of the structure under the satisfaction of constraints as the topological optimization evaluation index of the tensile monolithic structure. The expression of the objective function is:

$$f = \sum_{i=1}^{n_c} \rho_{ci} A_{ci} L_{ci} + \sum_{i=1}^{n_t} \rho_{ti} A_{ti} L_{ti} \tag{36}$$

The compression bar cross section A_{ci} can be determined by the following equation:

$$A_{ci} = \frac{2L_{ci}}{\gamma_c} \sqrt{\frac{T_{ci}}{\pi E}} \tag{37}$$

where: T_{ci} is the internal force of the ith compression bar in the self-equilibrium state of the structure at the current prestress level; γ_c is the safety factor of the strength of the compression bar; and E is the modulus of elasticity of the material.

The tension cable cross-sectional area A_{ti} is determined by the following equation:

$$A_{ti} = \frac{\gamma_R T_{ti}}{f_t} \tag{38}$$

where: T_{ti} is the internal force of the ith tie in the self-equilibrium state of the structure, γ_R is the fractional coefficient of tie resistance, and f_t is the design value of the strength of the tie material.

3.2.2 Handling of constraints

The problem of constraints is dealt with by the penalty function method, i.e., for an individual whose computational results do not satisfy the constraints, a penalty function is added to the value of its objective function to reduce the fitness of the individual in order to reduce the chance of the individual being inherited to the next generation.

In order to ensure that the nodes have the possibility of maintaining equilibrium stability under any spatial configuration and loading, the number of connected bars constraints need to be satisfied for all nodes. The node connected bars number constraint can be expressed as:

$$g_1 = \begin{cases} C_1 & \left(n_{\min} < 4\right) \\ 0 & \left(n_{\min} \geq 4\right) \end{cases} \tag{39}$$

where: g_1 denotes the constraint on the number of rods connected at nodes, C_1 is the penalty function term added to the objective function when an individual does not satisfy the condition on the number of rods connected at nodes, and $n_{\min}$ denotes the node with the lowest number of rods connected among all nodes, the constraint shows that under any topological relationship, at least four rods should be connected at each node of the tensioned monolithic structure. The compression rods in the tensile monolithic structure described in this paper can be continuous.

Under the given topological relationship, the corresponding self-equilibrium state of the tensioned monolithic structure can be found, requiring the maximum nodal unbalance force $F_{\max} \leq 10^{-3}\mathrm{N}$, then the constraint that the structure exists in a self-equilibrium state can be expressed as:

$$g_2 = \begin{cases} C_2 & \left(F_{\max} > 10^{-3} N\right) \\ 0 & \left(F_{\max} \leq 10^{-3} N\right) \end{cases} \tag{40}$$

where: g_2 indicates that the structure exists in the self-equilibrium state constraints, C_2 for when the individual does not meet the structure exists in the self-equilibrium state conditions added to the penalty function term.

In order to ensure the practical feasibility of the structure, the individual to find the self-equilibrium state of the structure, need to meet any two rods in addition to the nodes, in the other space location does not cross the collision, the rods do not cross the constraints can be expressed as:

$$g_3 = \begin{cases} C_3 & \left(d_{i,j} \leq d_{i,j,\min}\right) \\ 0 & \left(d_{i,j} > d_{i,j,\min}\right) \end{cases} \tag{41}$$

where: g_3 denotes the constraint of rod non-crossing, C_3 is the penalty function term added to an individual when it does not satisfy the condition of rod non-crossing, $d_{i,j}$ denotes the actual spatial distance between any two rods i and rods j of an individual in self-equilibrium, and $d_{i,j,\min}$ denotes the spatial distance between rods i and rods j. limit value, which can be determined by the following equation:

$$d_{i,j,\min} = \frac{\sqrt{A_i} + \sqrt{A_j}}{\sqrt{\pi}} \tag{42}$$

where: A_i, A_j indicate the cross-sectional area of rod i and rod j respectively.

When the overall structure of the tension structure and the combination of the dome structure, can be composed of a complete self-balancing tension structure, at this time the overall structure of the tension structure is subjected to the main force for the dome outside the ridge cable and the radial tensile force outside the diagonal cable. Provides that the tensioned overall structure in the radial force under the action of the inner span change, that is, the maximum internal radial displacement, can not exceed 1/800 of the structural span, the radial stiffness of the overall structure of the tensioned structure to meet the conditions of the following displacement limit:

$$g_4 = \begin{cases} C_4 & \left(u_{\max} > D/800\right) \\ 0 & \left(u_{\max} \geq D/800\right) \end{cases} \tag{43}$$

Stress conditions include 1) rod and cable stresses not exceeding the limits and 2) internal forces in the cable unit greater than zero, i.e., the cable should not slacken out of work. The stress constraints can be expressed as:

$$g_{5-1} = \begin{cases} C_{5-1} & \left(\text{Does not satisfy stress condition 1}\right) \\ 0 & \left(\text{Satisfies stress condition 1}\right) \end{cases} \tag{44}$$

$$g_{5-2} = \begin{cases} C_{5-2} & \left(\text{Does not satisfy stress condition 2}\right) \\ 0 & \left(\text{Satisfies stress condition 2}\right) \end{cases} \tag{45}$$

where: g_{5-1}, g_{5-2} denote the stress constraints under load, and C_{5-1}, C_{5-2} are the penalty function terms added to the objective function when an individual does not satisfy the stress constraints, respectively.

Therefore, the final expression of the objective function is:

$$h = f + g_1 + g_2 + g_3 + g_4 + g_{5-1} + g_{5-2} \tag{46}$$

where: h denotes the value of the objective function of the individual after the constraints have been processed.

3.3 Implementation of topology optimization based on small habitat genetic algorithm

3.3.1 Establishment of the Adaptation Function

The global minimum problem of the objective function can be converted into a global maximum problem suitable for genetic algorithm solution by using the conversion of the fitness formula considering the value of the objective function of each individual in the form of sorting from the largest to the smallest. The fitness calculation formula is:

$$Fit_i = 2 \times (k_i - 1) / (M - 1) \tag{47}$$

where: Fit_i denotes the fitness of individual i in the population, k_i is the ordinal number of individual i when all the individuals in the population are sorted by the value of their objective function from the largest to the smallest, and M is the total number of individuals in the population.

3.3.2 Computational model processing

The topological connectivity of the tensioned overall structure is randomly generated using a binary code, i.e., 0-1 encoding, with 1 indicating the presence of the corresponding bar and 0 indicating the absence of the corresponding bar.

3.3.3 Specific steps of the algorithm

The topology optimization of the overall structure of the tension can be carried out by using the small habitat genetic algorithm and combining it with the SMFF method. Fig. 2 shows the computational flow, where T is the number of generations of population evolution. The termination conditions in the flowchart are: 1) the evolutionary generations reach the maximum iteration value; 2) no more better individuals appear in 100 consecutive generations. If one of the termination conditions is satisfied, the calculation is terminated and the results are output.

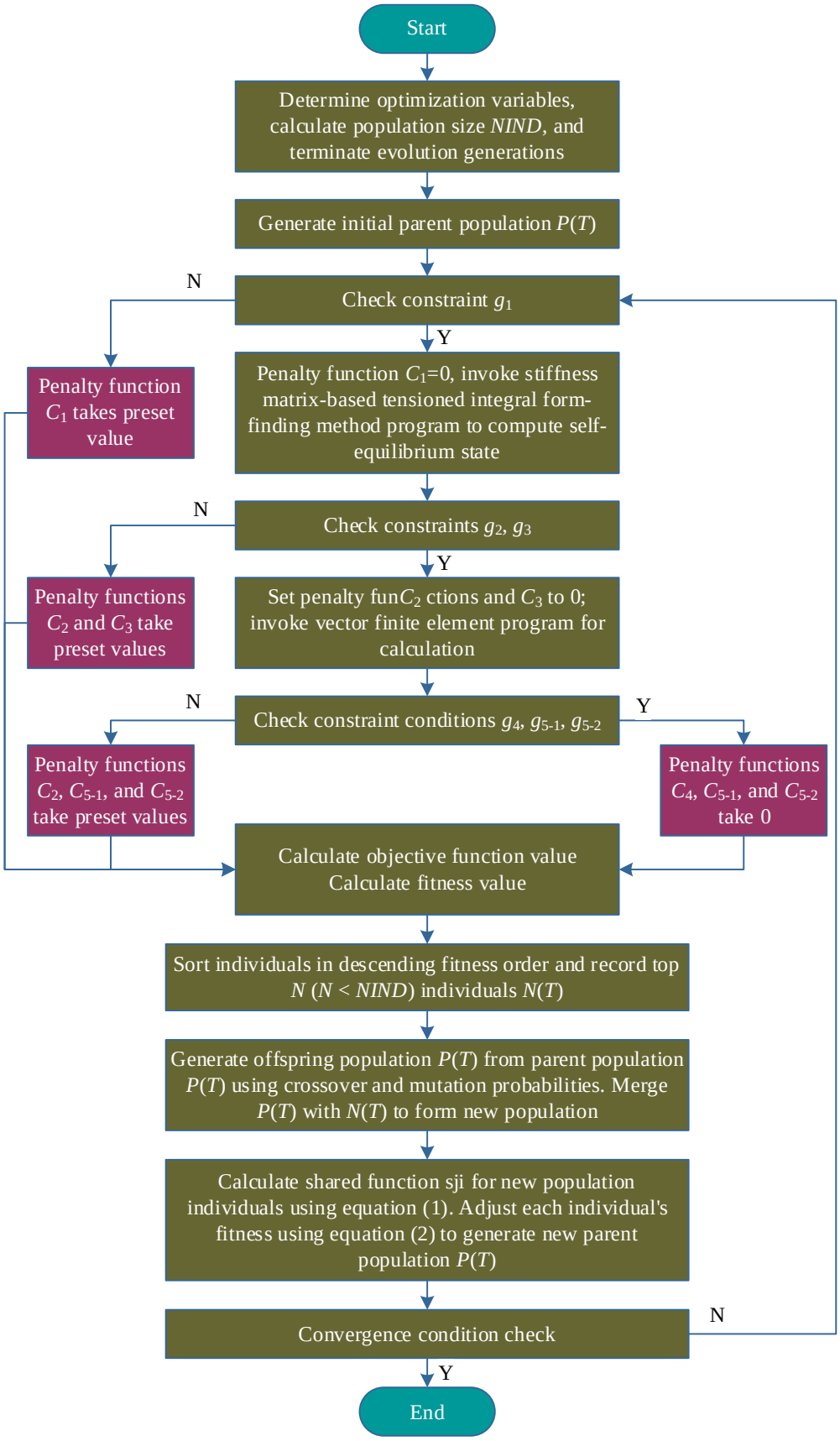

Figure 2: Flowchart of calculation steps

4 Influence of loading on the stiffness of the tensioned monolithic structure

The applied positions of the external loads of the quadrangular tensioned monolithic structure are categorized into five cases from position 1 to position 5, which are equally distributed at nodes N5~N8, node N5, node N6, node N7, and node N8, respectively.The influence of the positions of the loads on the stiffness of the tensioned monolithic structure in the absence of redundant constraints is investigated in terms of the load-displacement curves and the load-stiffness curves.

4.1 Load-Displacement Curve Analysis

In order to explore the influence of load location on the stiffness of the tensioned monolithic structure, the change rule of the load-displacement curves of each node is analyzed from X, Y and Z directions respectively. The load-displacement curves of each node of the four-pronged tensioned monolithic structure in the X, Y and Z directions are shown in Figs. 3 to 5, and the displacements in each direction corresponding to these nodes under the external load of 9.7kN are listed in Tables 1 to 3 respectively. In the load displacement curves in the X-direction of the structure, the laws of nodes N2 and N5, and the laws of N3, N4 and N7 are the same, so the X-direction load displacement diagrams of nodes N5, N6, N7, and N8 are shown in Fig. 3, and Figs. (a) to (d) are the X-direction load displacements of nodes N5, N6, N7, and N8, respectively, and the maximum X-direction node displacements of the quadrangular tensioned monolithic structure are shown in Table 1.

From Fig. 3 and Table 1, it can be seen that the X-direction displacement of node N5 is always the smallest among all the nodes when the external load is applied at five positions. The trends of the displacement curves of nodes N6 and N8 when the external load is applied at positions 3 and 5 are extremely similar, but there is a counterclockwise micro-rotation of the structure when it is applied at position 3, and the displacement of node N6 occurs in the X-positive direction, and that of node N8 in the X-negative direction, and the direction is reversed when it is applied at position 5.

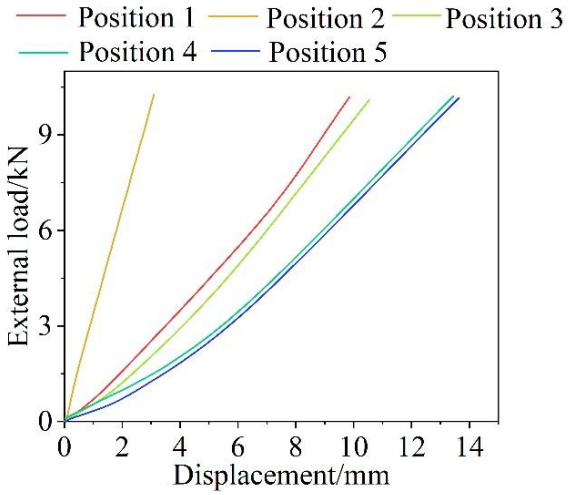

(a) The x direction of N5 is shifted

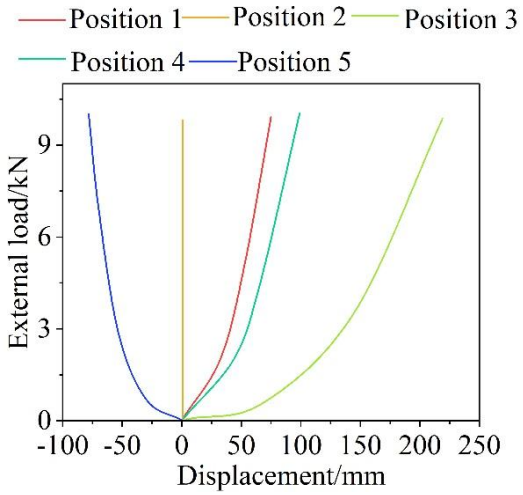

(b) The x direction of N6 is shifted

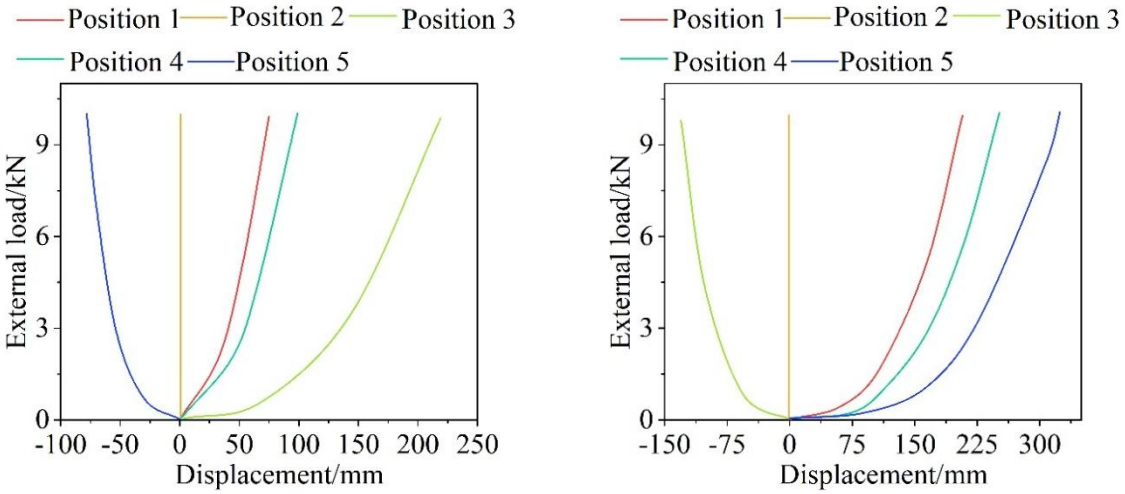

(c) The x direction of N7 is shifted (d) The x direction of N8 is shifted

Figure 3: The x direction load displacement of the node

Table 1: X direction node maximum displacement (mm)

Node number	Position 1	Position 2	Position 3	Position 4	Position 5
N2	2.93	1.19	3.07	3.87	3.81
N3	267.10	2.22	64.96	335.48	242.88
N4	265.59	2.37	63.25	332.93	240.27
N5	9.75	3.15	10.48	13.37	13.53
N6	64.52	2.45	198.00	86.63	-75.85
N7	261.26	2.90	58.44	325.92	232.83
N8	207.17	3.54	-127.82	252.83	323.44

Figure 4 and Table 2 respectively show the Y-direction load-displacement curve of the node and the maximum displacement of the node in the Y-direction of the structure. Figures (a) to (d) respectively show the Y-direction load-displacement of nodes N5, N6, N7, and N8. The displacement curve trends of each pair of nodes N5 and N7, and N6 and N8 are all symmetrical about the X=0 axis, that is, no matter at which position the external load is applied, The node displacements of the structure in the Y direction show the characteristic that the changes of N5 and N7 are symmetrical about the X=0 axis, and the same is true for N6 and N8. During the stressing process, the displacements of N6 are all in the positive direction of Y, while the displacements of N8 are all in the negative direction. Node N5 produces displacement in the negative direction of Y when external load is applied at position 3, but all displacements in the positive direction of Y are produced when external load is applied at other positions; node N7 produces displacements in the exact opposite direction to N5. From this, it can be learned that the displacements of the structure in the Y direction of the nodes at symmetric positions are reverse symmetric.

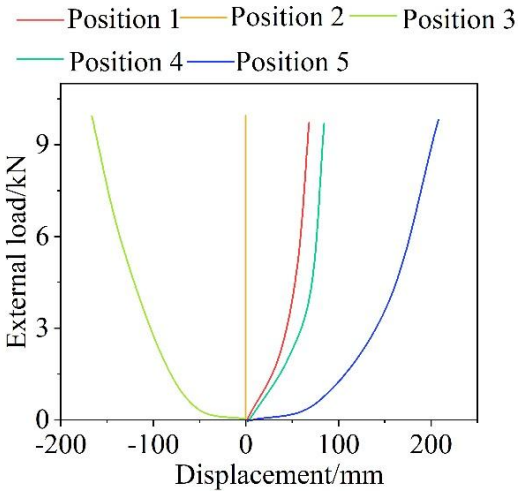

(a) The y direction of N5 is shifted

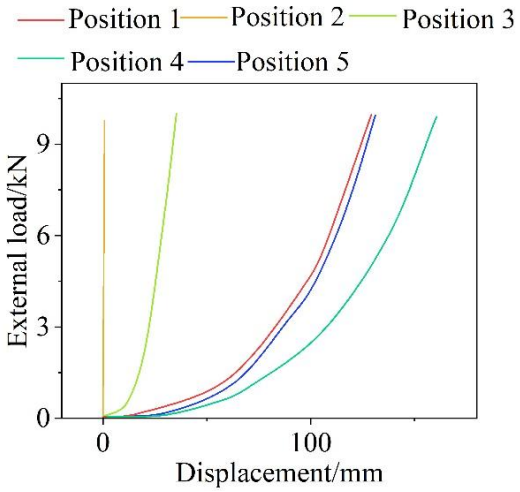

(b) The y direction of N6 is shifted

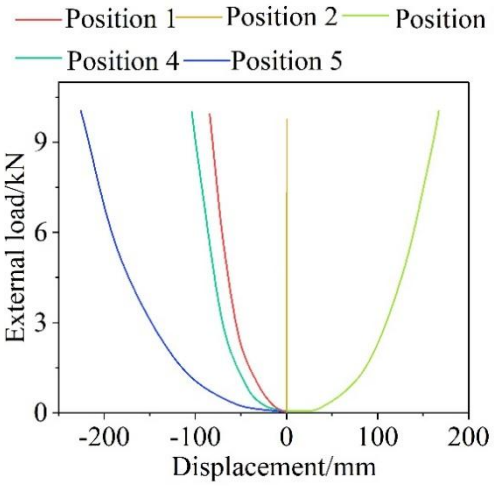

(c) The y direction of N7 is shifted

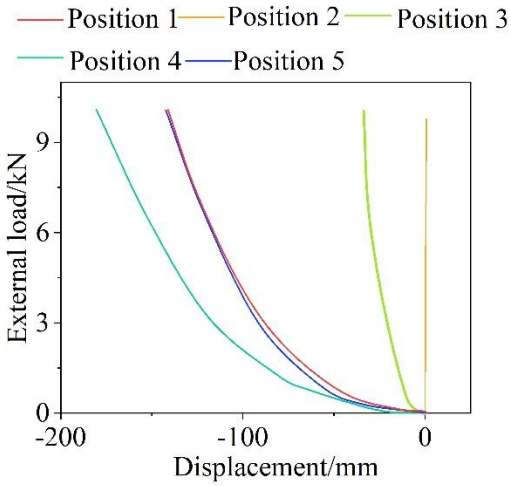

(d) The y direction of N8 is shifted

Figure 4: The y direction load displacement of the node

Table 2: Y direction node maximum displacement (mm)

Node number	Position 1	Position 2	Position 3	Position 4	Position 5
N2	0	0	0	0	0
N3	0	0	0	0	0
N4	-10.24	-0.16	1.65	-16.12	-7.76
N5	-10.36	-0.21	0.94	-16.39	-7.24
N6	74.86	0.13	-166.72	88.09	219.35
N7	130.52	0.18	35.01	163.24	132.36
N8	-86.21	-0.94	167.71	-105.35	-228.36

Regarding the Z-direction displacement curves, the change trends of nodes N5 and N7, N6 and N8 are identical and numerically close to each other. Fig. 5 shows the node Z-direction load-displacement curves, and Figs. (a) and (b) are the Z-direction load-displacements of nodes N5 and N6, respectively. Table 3 shows the maximum node displacements of the quadratic tensile monolithic structure in the Z-direction, and the nodes N5 and N7 produce positive Z-

direction displacements at the rest of the positions. When the external load is applied at position 3, the nodes N5 and N7 are displaced in the positive Z-direction, and the remaining positions are displaced in the negative direction. When the external load is applied at position 5, the nodes N6 and N8 produce negative Z-direction displacements, and the remaining positions produce positive displacements. When the external load is applied at position 2, the Z-direction displacement of each node is within 2mm. It can be learned that the Z-direction displacement curves of the nodes in the symmetric position of the structure maintain a consistent trend.

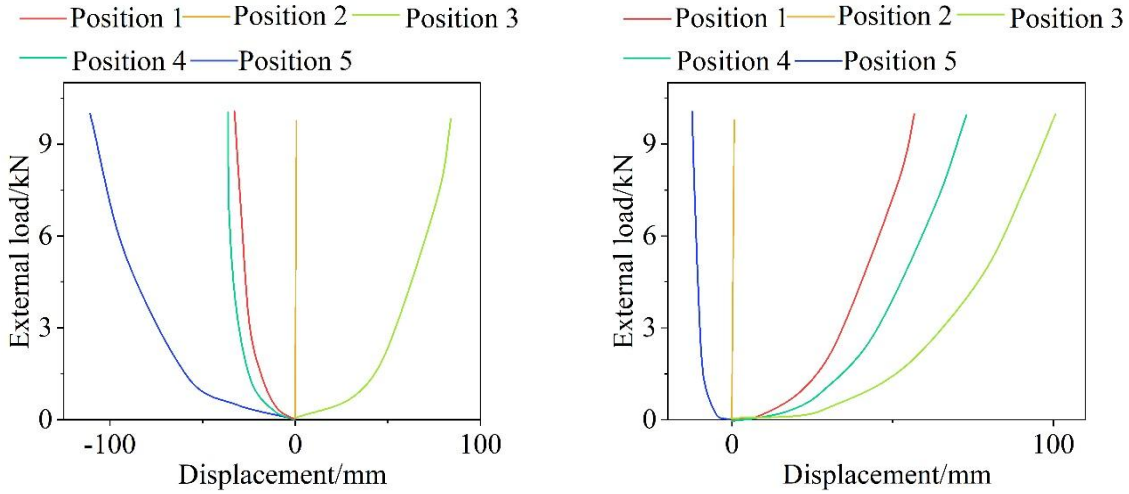

(a) The z direction of N5 is shifted (b) The z direction of N6 is shifted

Figure 5: The z direction load displacement of the node

Table 3: Z direction node maximum displacement (mm)

Node number	Position 1	Position 2	Position 3	Position 4	Position 5
N5	-31.78	1.84	84.75	-36.14	-110.19
N6	56.84	0.16	100.56	73.64	-12.00
N7	-34.85	-1.00	82.07	-39.17	-113.42
N8	55.53	-0.87	98.82	72.52	-13.50

4.2 Load-Stiffness Curve Analysis

The structural load-stiffness curves are shown in Fig. 6, and Figs. (a) and (b) show the structural load-stiffness curves covering position 2 and not covering position 2, respectively, and the magnitude of the structural stiffnesses when the external loads are applied at different positions are shown in Table 4.

The load-stiffness curves show that the structural stiffness increases as the external load increases. The stiffness of the structure also changes depending on the location of the external load. In the longitudinal comparison of the load-stiffness curve, under the action of the same size of the external load, the stiffness of the external load applied at position 2 is the largest, which is much larger than the structural stiffness in other cases, but the external load increases to 9.4218kN when the internal force of some of its rods is reduced to 0, and at this time, the structure no longer has stiffness.

Under the influence of the applied position of the external load, the size of the stiffness is ranked as Position 2 > Position 3 > Position 5 > Position 1 > Position 4, in which the stiffness of the external load applied at Position 2 and Position 4 is the largest and the smallest, respectively, due to the fact that the nodes N5 and N7 are the tensile and compressive ends,

respectively, for the structural bending of the force. Position 3 > position 5 is the change in magnitude of the structural stiffness due to the relative position of nodes N6 and N8 in the direction of clockwise rotation of the structural unit.

Through the above effects of the load action position on the four-pronged tensile integral structure, analyzing the change rule of the load-displacement curve, the load-internal force curve, and the load-stiffness curve, it can be learned that:

(1) The load-displacement curve of the structure has more obvious nonlinear characteristics in the initial stage of just applying external load. There is also a symmetrical law in the direction of the displacement of the nodes symmetrical about the diagonal on the top surface of the structure.

(2) The load-internal force curves of the structure show different characteristics when the external load is applied at position 2. All cases except position 2 show a nonlinear increase in the internal force of the bars with the increase of the external load, and the stiffness of the structure also increases.

(3) The load-stiffness curves of the structure show that the structural stiffness increases with the increase of the external load, and the structural stiffness changes due to the different positions of the external load.

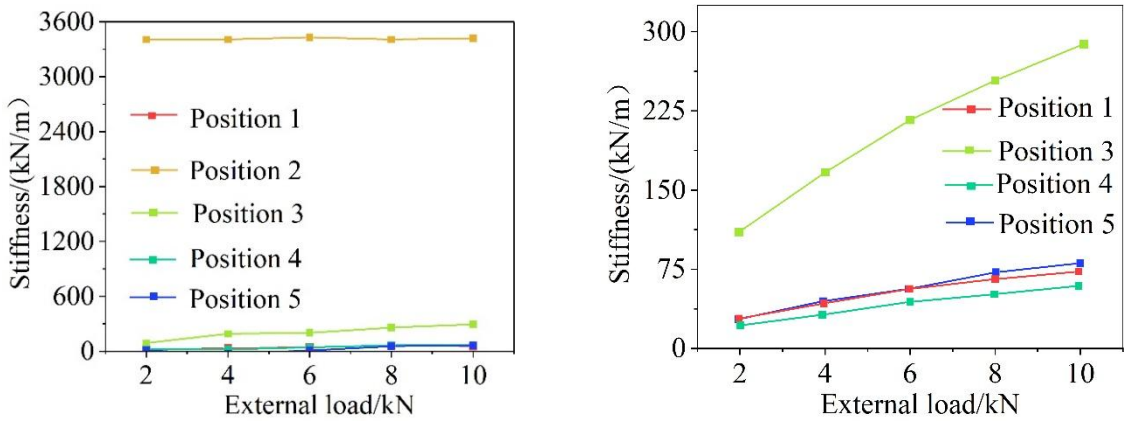

(a) Cover location 2 (b) No location 2

Figure 6: Structural load - stiffness curve

Table 4: The overall structural stiffness of the four-prism tension

Outer load size	Position 1	Position 2	Position 3	Position 4	Position 5
2kN	27.7063	3340.5343	110.3265	21.4224	28.0827
4kN	41.9543	3341.0257	166.3972	33.0138	44.0696
6kN	53.7780	3341.5166	212.0423	42.6450	57.6180
8kN	64.2159	3342.0089	251.7395	51.1639	69.7793
10kN	73.7046	--	287.3641	58.9245	80.9847

5 Analysis of the results of the optimization of the topology of the tensile monolithic structure

5.1 Example analysis

The following tensioned monolithic structure has a total of 12 nodes, each of which is connected to 6 members, with a total of 12 compression rods (green color) and 24 tension ropes (black

color), and the topological connection of the structure is shown in Fig. 7. The structure is a multi-self-stress modal structure, so there are many possibilities for its initial force density. To solve the initial force density of this tensioned monolithic structure using the small habitat genetic algorithm proposed in this paper, the members need to be grouped according to the geometric symmetry of the structure beforehand. Different grouping situations may lead to different results in finding the shape of the initial force density.

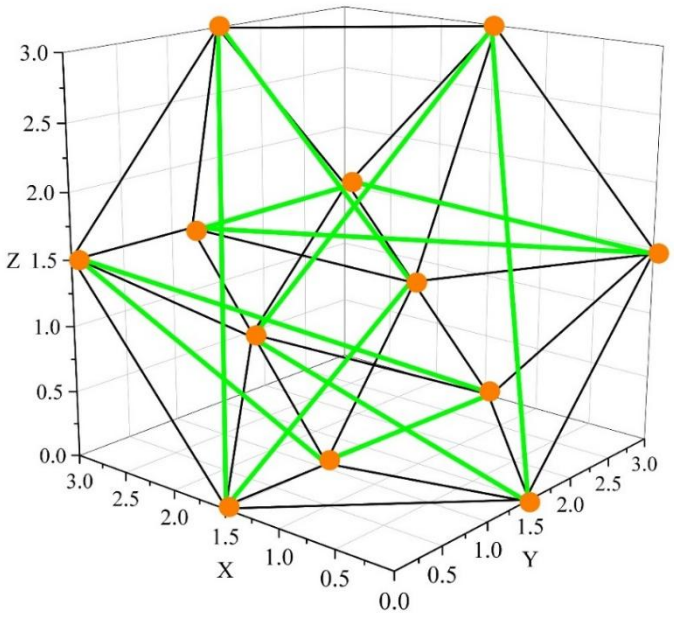

Figure 7: Structural topology connection

According to the geometric symmetry, the cable unit is divided into 4 groups and the rod unit is divided into 1 group, the specific grouping is shown in Fig. 8, and the solution results are shown in Table 5. The structure in this symmetric grouping state there is a unique initial force density, and with the genetic algorithm based on the geometrically symmetric tensioning of the overall structure of the shape finding method solution results are consistent, which design error k = $1.8685e^{-1}$ to meet the design requirements. However, the finding result of the genetic algorithm based finding method is single. This paper can solve a variety of initial force density results according to different symmetric grouping, which is the advantage of this paper's algorithm. Under the action of the above initial force density, the stability of the structure can be considered, in which the tangential stiffness matrix eigenvalues are shown in Table 6, from which it can be seen that the smallest eigenvalue is positive, with a value of 15.415, which means that the structure is in a stable state.

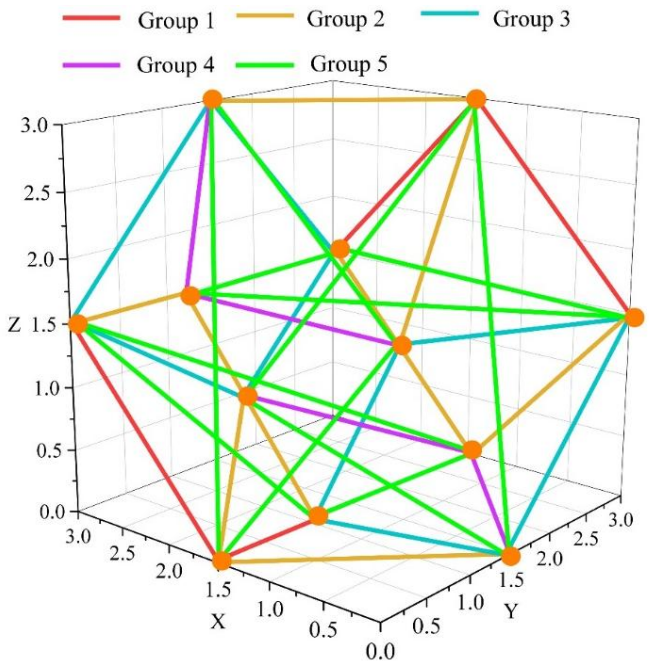

Figure 8: Specific grouping results (h=5)

Table 5: The result of the solution (h=5)

Group	Unit	The force density of this article	A method based on genetic algorithms
Group1	1~4	1.000	1.005
Group2	5~12	0.550	0.550
Group3	13~20	0.550	0.550
Group4	21~24	1.000	1.005
Group5	25~36	-0.515	-0.515

Table 6: Characteristics of the stiffness matrix of 12 bar tension (h=5)

Eigenvalue number	eigenvalue
λ_1	15.415
λ_2	41.212
λ_3	82.546
λ_4	88.651
λ_5	88.651
λ_6	92.544
.....	.....
λ_{36}	1745.126

In order to further elaborate the advantages of the algorithm in this paper and show the solving ability of multiple initial force density states, the overall structure of the spatial 12-bar tensioning can be divided into 12 groups, and the specific grouping is shown in Figure 9. The grouping has a variety of initial force density, so it is necessary to optimize the standard deviation of force density of grouped components as the objective function, and the optimization results are shown in Table 7, and the error value of $k = 7.475e^{14}$ is obtained, which meets the design requirements.

The eigenvalue statistics results are shown in Table 8, comparing the two grouping results, due to the different grouping, the final value of the force density will be changed, the minimum

eigenvalue of the tangent stiffness matrix of the structure in the case of h = 5 is still positive, so it can be ensured that the structure is still in a stable state under the action of the force density, and meanwhile, in the case of the 12-component grouping (h = 12), the structure forms a slightly better stiffness than the 5-component grouping (h = 12), which meets the condition of the structural stability. At the same time, the stiffness of the structure formed in the case of 12-component group (h = 12) is slightly better than that of the structure with 5-component group (h = 5).

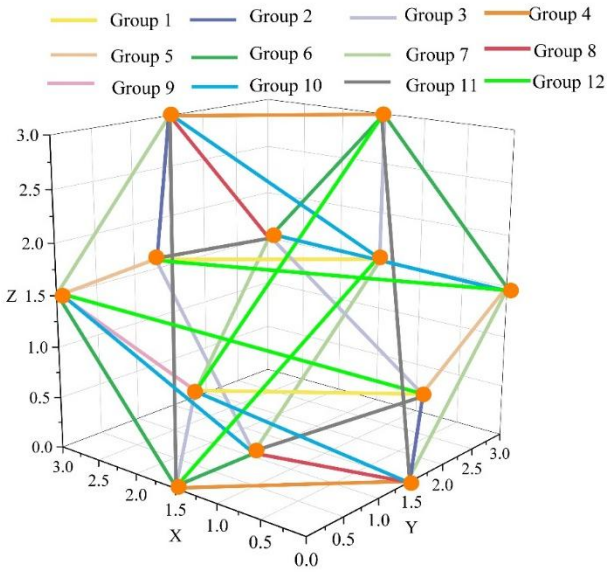

Figure 9: Specific grouping(h=12)

Table 7: The initial force density of the whole structure of the tensia is (h=12)

Group	Unit	The force density of this article	Group	Unit	The force density of this article
Group1	1~2	1.000	Group7	17~20	0.446
Group2	3~4	0.785	Group8	21~22	0.342
Group3	5~8	0.396	Group9	23~24	0.553
Group4	9~10	0.505	Group10	25~28	0.448
Group5	11~12	0.505	Group11	29~32	0.395
Group6	13~15	0.895	Group12	33~36	0.505

Table 8: Characteristics of the stiffness matrix of 12 bar tension (h=12)

Eigenvalue number	eigenvalue
λ_1	18.519
λ_2	43.216
λ_3	84.845
λ_4	91.782
λ_5	91.805
λ_6	97.944
.....	.....
λ_{36}	1746.025

The structural grouping is now increased to 36 groups, that is, a single member for a group, through the calculation of the self-stress modal number and the self-stress modal number s is the same as the ungrouped self-stress modal number, it shows that the method of grouping the members does not play a role in reducing the self-stress modal number. However, the purpose of grouping at this time is only to determine the tension-pressure relationship within the structure, which ensures that the calculation results meet the tension-pressure relationship of the structural members. The initial force density value finally obtained is calculated with a design error of $k = 8.8944e^{-14}$, and the specific force density values are shown in Table 9.

At the same time, the stability of the structure needs to be calculated, the solution obtained tangent stiffness minimum eigenvalue of 20.443, which is greater than 0, it means that the structure is stable, the specific data shown in Table 10. The case of a single member for each group is also consistent with the asymmetric structure of the group solution. Therefore, the algorithm of this paper can also be applied to the initial force density solution of asymmetric structures.

Table 9: The initial force density of the whole structure of tensia is (h=36)

Group	Unit	The force density of this article	Group	Unit	The force density of this article
Group1	1	1.000	Group19	19	1.815
Group2	2	0.754	Group20	20	1.336
Group3	3	0.637	Group21	21	0.694
Group4	4	0.398	Group22	22	0.694
Group5	5	1.214	Group23	23	0.694
Group6	6	1.556	Group24	24	0.694
Group7	7	1.556	Group25	25	-0.556
Group8	8	1.212	Group26	26	-0.815
Group9	9	0.754	Group27	27	-0.815
Group10	10	1.000	Group28	28	-0.556
Group11	11	40.395	Group29	29	-0.556
Group12	12	0.632	Group30	30	-0.845
Group13	13	1.000	Group31	31	-0.556
Group14	14	0.755	Group32	32	-0.815
Group15	15	0.635	Group33	33	-0.512
Group16	16	0.398	Group34	34	-0.512
Group17	17	1.455	Group35	35	-0.878
Group18	18	0.981	Group36	36	-0.878

Table 10: Characteristics of the stiffness matrix of 12 bar tension (h=36)

Eigenvalue number	eigenvalue
λ_1	20.443
λ_2	44.925
λ_3	87.644
λ_4	95.025
λ_5	95.216
λ_6	102.194
.....	.....
λ_{36}	1746.624

5.2 Evaluation of topologically optimized morphology

Since designers may prefer to focus on a certain characteristic of the structure in the process of structural design, the function distinguishes the primary and secondary relationship of each characteristic in the structural design by setting the weight coefficients. At the same time, it can effectively demonstrate the relationship between the coefficients and the comprehensive evaluation index by combining the three coefficients of α,β, α,γ and β,γ, where α, β and γ are the weight coefficients of the design objectives of stiffness maximization, weight minimization and stress minimization, respectively, which is convenient for the designer to judge the superior interval of the various structural performances. Figure 10~Figure 12 show the comprehensive evaluation results of the three combinations of weight coefficients, respectively.The relationship between the comprehensive evaluation indexes and the weight coefficients of the three multi-autostress modal tensioned monolithic structures is presented as three spatial triangular planes, which reflect the corresponding comprehensive evaluation functions of the three topological configurations. And from the three spatial triangular planes top views, the optimal applicable areas between different structures under various combinations can be seen. α,β, α,γ and β,γ top views of the three spatial triangular planes with different combinations of coefficients are shown in Fig. 10 to Fig. 12, respectively.

It can also be found that the ratio of area reflects the probability of obtaining the comprehensive performance optimization of the corresponding topological configuration under the three combinations of weight coefficients. For example, the structure with the largest area ratio is the grouping structure of h=12, followed by the grouping structure of h=5 and the grouping structure of h=36. At this time, it indicates that the grouping structure of h=12 is more likely to obtain the optimal comprehensive evaluation value compared with the grouping structure of h=5 and the grouping structure of h=36. When the combination of weight coefficients is replaced, the dominant regions of all three structures change. However, it is worth noting that no matter how the three combinations of weight coefficients are changed, the area of the dominant regions of the three structures will remain the same, and the area ratios of the three regions (the grouping structure of h=12, the grouping structure of h=5, and the grouping structure of h=36) are 59.25%, 30.33%, and 10.42%, respectively. Therefore, when dealing with situations where there is no special need, it is recommended that designers prioritize the use of the grouping structure with h=12 because it has better structural advantages than the other two structures. In addition, it is recommended that the value of the weight coefficients needs to be adjusted in cases where more attention is paid to the structural properties, such as low elastic strain energy or greater structural stiffness, and then based on the comprehensive evaluation of the resultant plots, in order to find a suitable topological configuration.

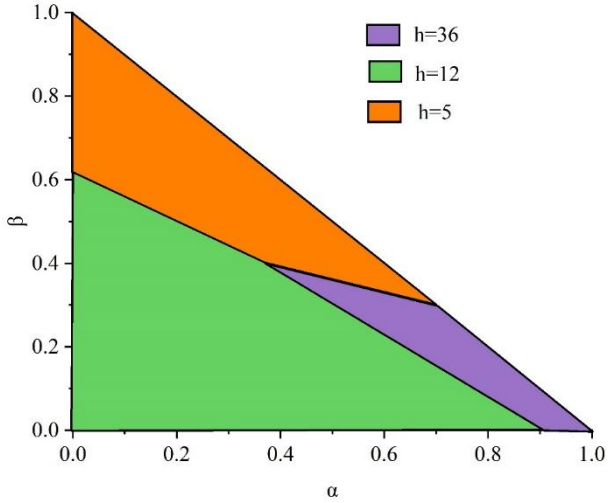

Figure 10: The spatial triangle plane is in the view of α,β

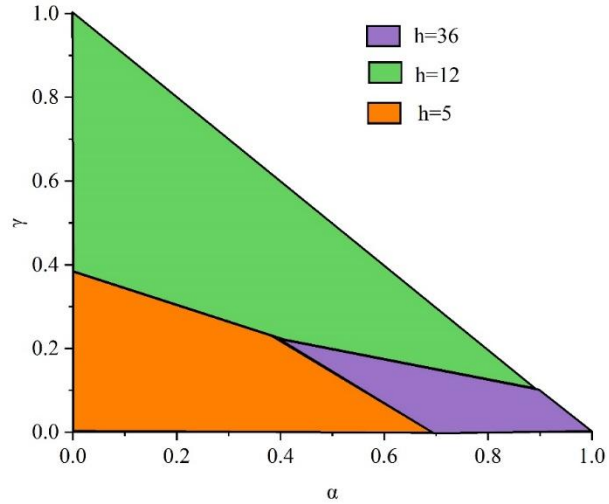

Figure 11: The spatial triangle plane is in the view of α,γ

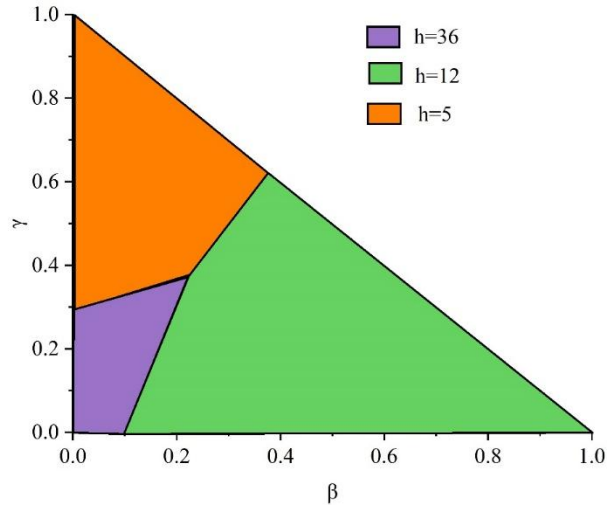

Figure 12: The spatial triangle plane is in the view of β,γ

5.3 Parameter sensitivity analysis

From the above studies, it is obvious to conclude that the composite evaluation value is directly affected by the weighting coefficients, therefore, the parameter sensitivity analysis is necessary in the study of the effects of different parameters on the structural performance.

In this section, the spatial angle formed by any triangular plane (grouped structure with h=5, grouped structure with h=12, grouped structure with h=36) and the bottom plane is taken as the comparative index of parameter sensitivity, and the spatial angle formed by each plane and the bottom plane will react to the degree of inclination of the plane, i.e., it reacts to the rate of change of the comprehensive evaluation value with the change of coefficients. The space angle of each plane under different combinations of coefficients is obtained by spatial geometry theory calculation, and the spatial angle of the plane in the topological morphology evaluation diagram is shown in Figure 13. With different combinations of arbitrary weighting coefficients, the spatial angle of the corresponding plane of the grouping structure with h=12 is the smallest relative to the other two cases, indicating that the weighting coefficients have the smallest influence on the comprehensive evaluation value. In other words, with the same combination of weighting coefficients, this structure has the lowest sensitivity and the strongest robustness. In contrast, the grouping structure with h = 5 corresponds to the largest spatial angle of the plane, indicating that the composite evaluation value of this structure is easily swayed by the change of weight coefficients. Therefore, this structure has high sensitivity and weakest robustness under the same combination of weighting coefficients.

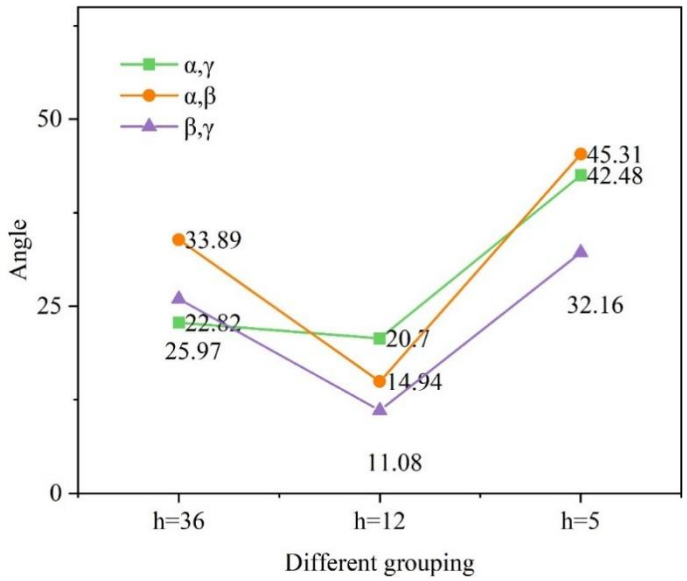

Figure 13: The planar space Angle in the topological form evaluation diagram

When the weight coefficients of a certain item are consistent, the sensitivity of the same structure to two other different weight coefficients is obtained by means of formula derivation. The following is an example of theoretical derivation in the case of consistent coefficients before β:

The space triangular plane equation can be abbreviated as:

$$\alpha k_1 + \beta k_2 + \gamma k_3 - G = 0 \tag{48}$$

and can be defined as k_1, k_2, k_3:

$$k_1 = 1 - \frac{h_\eta}{\sum_{\eta=1}^{N} h_\eta} \tag{49}$$

$$k_2 = 1 - \frac{U_\eta}{\sum_{\eta=1}^{N} U_\eta} \tag{50}$$

$$k_3 = \frac{\lambda_{\min,\eta}}{\sum_{\eta=1}^{N} \lambda_{\min,\eta}} \tag{51}$$

At the same time α, β, γ is satisfied:

$$\alpha + \beta + \gamma = 1 \tag{52}$$

Thus with α, β as the combination of coefficients, the above equation (52) can be deformed as:

$$\alpha(k_1 - k_3) + \beta(k_2 - k_3) - G + k_3 = 0 \tag{53}$$

Since the structural properties of any structure are certain, here k_1, k_2, k_3 are fixed and the normal vector of the space plane can be obtained as $(k_1 - k_3, k_2 - k_3, -1)$, and let the normal vector of the bottom plane be $(0,0,1)$:

$$\cos\varphi_{\alpha,\beta} = \frac{1}{\sqrt{(k_1 - k_3)^2 + (k_2 - k_3)^2 + 1}} \tag{54}$$

where $\varphi_{\alpha,\beta}$ is the angle between the plane and the base plane for the combination of the coefficients of α, β.

Similarly, in the case of the combination of coefficients of β, γ, the spatial plane equations can be similarly rewritten as:

$$\beta(k_2 - k_1) + \alpha(k_3 - k_1) - G + k_1 = 0 \tag{55}$$

The plane normal vector can also be obtained as $(k_2 - k_1, k_3 - k_1, -1)$, so the cosine of the angle between the plane and the base can be obtained for a combination of β, γ coefficients:

$$\cos\varphi_{\beta,\gamma} = \frac{1}{\sqrt{(k_2 - k_1)^2 + (k_3 - k_1)^2 + 1}} \tag{56}$$

where $\varphi_{\beta,\gamma}$ is the angle between the plane and the bottom surface under the combination of β, γ coefficients.

The solution results of the three structures are consistent with $\varphi_{\alpha,\beta} > \varphi_{\beta,\gamma}$, and according to the above equations, we get $\cos\varphi_{\beta,\gamma} > \cos\varphi_{\alpha,\beta}$, so $k_2 - k_3 > k_2 - k_1$. To ensure that the β pre-coefficients are consistent, the α pre-coefficients in the case of α, β combinations are $\frac{k_1 - k_3}{k_2 - k_3}$ and the γ pre-coefficients are $\frac{k_3 - k_1}{k_2 - k_1}$. Therefore the γ-prior coefficient is greater than the α-prior coefficient, at which point the structure is shown to be more sensitive to γ.

6 Conclusion

On the basis of previous research, this paper finds that there are still deficiencies in the theory of topology finding of tensile integrated structure, so it aims at the sensitivity of the stiffness matrix and optimization of the design of the key issues to carry out research. The design method of the tensioned overall structure is optimized based on small habitat genetic algorithm, which provides a certain theoretical basis and technical support for the topological shape finding and optimization of the tensioned overall structure.

(1) In the tensile monolithic structure of four-pronged column, the stiffness changes regularly with different load positions. The order of influence is position 2>position 3>position 5>position 1>position 4. The load-displacement curves show obvious nonlinearity in the early loading stage, and the displacement response of the symmetric nodes shows the characteristics of synergistic or reverse symmetry, which indicates that the geometrical symmetry of the structure plays a dominant role in the mechanical response.

(2) In this paper, the topology optimization of tensile monolithic structure based on small habitat genetic algorithm has excellent solving ability for geometrically symmetric tensile monolithic structure, and it is also applicable to solving the initial force density of asymmetric structure. The topology optimization algorithm of the tensioned monolithic structure based on the small habitat genetic algorithm divides the spatial twelve-bar tensioned monolithic structure components into five, twelve, and thirty-six groups, and carries out the optimization in groups respectively. After optimization, the eigenvalues of the tangent stiffness matrix of the stress density are positive, and the structure is in a stable state, which confirms that the topology optimization algorithm of the tensioned overall structure based on the small habitat genetic algorithm can effectively solve the initial force density of the tensioned overall structure.

(3) The sensitivity analysis of the tensioned overall structure helps the designers to make comprehensive consideration of the topological morphology of the specific structure and select the appropriate topological morphology. In the comprehensive evaluation planes of different grouped structures, the grouped structure with h=12 has the best comprehensive performance, with the largest occupied area of 59.25%, and its sensitivity to the weight coefficients is the lowest, which has better comprehensive performance and design robustness.

References

[1] Schorr, P., Li, E. R. C., Kaufhold, T., Hernández, J. A. R., Zentner, L., Zimmermann, K., & Böhm, V. (2021). Kinematic analysis of a rolling tensegrity structure with spatially curved members. Meccanica, 56(4), 953-961.

[2] Skelton, R. E., Helton, J. W., Adhikari, R., Pinaud, J. P., & Chan, W. (2017). An introduction to the mechanics of tensegrity structures. In The mechanical systems design handbook (pp. 315-388). CRC Press.

[3] Liu, Y., Bi, Q., Yue, X., Wu, J., Yang, B., & Li, Y. (2022). A review on tensegrity structures-based robots. Mechanism and Machine Theory, 168, 104571.

[4] Gilewski, W., Kłosowska, J., & Obara, P. (2015). Applications of tensegrity structures in civil engineering. Procedia Engineering, 111, 242-248.

[5] Guest, S. D. (2011). The stiffness of tensegrity structures. IMA Journal of Applied Mathematics, 76(1), 57-66.

[6] Gomez-Jauregui, V., Quilligan, M., Manchado, C., & Otero, C. (2018). Design, fabrication and construction of a deployable double-layer tensegrity grid. Structural Engineering International, 28(1), 13-20.

[7] Zhang, X., Pei, Z., & Tang, Z. (2025). Research pathways from tensegrity-related biological structures to tensegrity robots: a bibliometric analysis. Bioinspiration & Biomimetics, 20(4), 041004.

[8] Lu, Z., Li, H. J., & Wang, C. (2020). Stability of cable-supported spherical reticulated shell with tension members. International Journal of Space Structures, 35(3), 69-79.

[9] Chen, B., & Jiang, H. (2021). Body stiffness variation of a tensegrity robotic fish using antagonistic stiffness in a kinematically singular configuration. IEEE Transactions on Robotics, 37(5), 1712-1727.

[10] Latteur, P., Feron, J., & Denoel, V. (2017). A design methodology for lattice and tensegrity structures based on a stiffness and volume optimization algorithm using morphological indicators. International Journal of Space Structures, 32(3-4), 226-243.

[11] Gilewski, W., & Al Sabouni-Zawadzka, A. (2020). Equivalent mechanical properties of tensegrity truss structures with self-stress included. European Journal of Mechanics-A/Solids, 83, 103998.

[12] Ali, N. B. H., & Smith, I. F. C. (2010). Dynamic behavior and vibration control of a tensegrity structure. International Journal of Solids and Structures, 47(9), 1285-1296.

[13] Tran, H. C., & Lee, J. (2010). Advanced form-finding of tensegrity structures. Computers & structures, 88(3-4), 237-246.

[14] Lee, S., Lee, J., & Kang, J. W. (2017). Results of generalized equilibrium path from form-finding of tensegrity structure. International Journal of Steel Structures, 17(3), 1225-1231.

[15] Zhang, P., Zhou, J., & Chen, J. (2021). Form-finding of complex tensegrity structures using constrained optimization method. Composite Structures, 268, 113971.

[16] Cai, J., & Feng, J. (2015). Form-finding of tensegrity structures using an optimization method. Engineering Structures, 104, 126-132.

[17] Gasparini, D., Klinka, K. K., & Arcaro, V. F. (2012). A finite element for form-finding and static analysis of tensegrity structures. Journal of Mechanics of Materials and Structures, 6(9), 1239-1254.

[18] Yuan, X. F., Ma, S., & Jiang, S. H. (2017). Form-finding of tensegrity structures based on the Levenberg–Marquardt method. Computers & Structures, 192, 171-180.

[19] Wang, Y., Han, Z., Xu, X., & Luo, Y. (2024). Topology optimization of active tensegrity structures. Computers & Structures, 305, 107513.

[20] Xu, X., Wang, Y., & Luo, Y. (2016). General approach for topology-finding of tensegrity structures. Journal of Structural Engineering, 142(10), 04016061.

[21] Liu, K., & Paulino, G. H. (2019). Tensegrity topology optimization by force maximization on arbitrary ground structures. Structural and Multidisciplinary Optimization, 59(6), 2041-2062.

[22] Ehara, S., & Kanno, Y. (2010). Topology design of tensegrity structures via mixed integer programming. International Journal of Solids and Structures, 47(5), 571-579.

[23] Feng, X., Zhang, W., Jianbo, S., Chen, Y., & Sergio, Z. (2021). The topology finding algorithm of tensegrity structures based on scheme matrix strategy. Composite Structures, 275, 114429.

[24] Lee, S., & Lee, J. (2016). A novel method for topology design of tensegrity structures. Composite Structures, 152, 11-19.

[25] Zhang, L. Y., Li, Y., Cao, Y. P., & Feng, X. Q. (2014). Stiffness matrix based form-finding method of tensegrity structures. Engineering structures, 58, 36-48.

[26] Boehler, Q., Abdelaziz, S., Vedrines, M., Poignet, P., & Renaud, P. (2017). From modeling to control of a variable stiffness device based on a cable-driven tensegrity mechanism. Mechanism and Machine Theory, 107, 1-12.

[27] Ashwear, N., Tamadapu, G., & Eriksson, A. (2016). Optimization of modular tensegrity structures for high stiffness and frequency separation requirements. International Journal of Solids and Structures, 80, 297-309.

[28] Luo, A., Cao, Z., Liu, H., & Feng, Y. (2023). Stiffness of three-bar tensegrity structure. Engineering Computations, 40(4), 823-835.

[29] Yildiz, K., & Lesieutre, G. A. (2019). Effective beam stiffness properties of n-strut cylindrical tensegrity towers. AIAA journal, 57(5), 2185-2194.

[30] Zappetti, D., Jeong, S. H., Shintake, J., & Floreano, D. (2020). Phase changing materials-based variable-stiffness tensegrity structures. Soft robotics, 7(3), 362-369.